Interannual Variability of the Sulawesi Sea Circulation Forced by Indo-Pacific Planetary Waves

Xiaoyue Hu, Janet Sprintall, Dongliang Yuan, Benoît Tranchant, Philippe Gaspar, Ariane Koch-Larrouy, Guillaume Reffray, Xiang Li, Zheng Wang, Yao Li, et al.

JGR Oceans

RESEARCH ARTICLE
10.1029/2018JC014356

Special Section:
Recent Progresses in Oceanography and Air-Sea Interactions in Southeast Asian Archipelago

Interannual Variability of the Sulawesi Sea Circulation Forced by Indo-Pacific Planetary Waves

Xiaoyue Hu[1,2,3,4], Janet Sprintall[5], Dongliang Yuan[1,2,3,4], Benoît Tranchant[6], Philippe Gaspar[6], Ariane Koch-Larrouy[7,8], Guillaume Reffray[8], Xiang Li[1,3,4], Zheng Wang[1,3,4], Yao Li[1,3,4], Dwiyoga Nugroho[9], Corry Corvianawatie[1,2,10], and Dewi Surinati[10]

[1]Key Laboratory of Ocean Circulation and Wave, Institute of Oceanology, Chinese Academy of Sciences, Qingdao, China, [2]University of Chinese Academy of Sciences, Beijing, China, [3]Qingdao National Laboratory for Marine Science and Technology, Qingdao, China, [4]Center for Ocean Mega-Science, Chinese Academy of Sciences, Qingdao, China, [5]Scripps Institution of Oceanography, University of California, San Diego, La Jolla, CA, USA, [6]Collecte Localisation Satellites (CLS), Ramonville Saint-Agne, France, [7]LEGOS, Toulouse, France, [8]Mercator Océan, Ramonville Saint-Agne, France, [9]Agency of Research and Development for Marine and Fisheries, MMAF, Jakarta, Indonesia, [10]Research Center for Oceanography, Indonesian Institute of Science, Jakarta, Indonesia

Abstract The regional INDESO model configured in the Indonesian seas from 2008 to 2016 is used to study the mechanisms responsible for the variability of the currents in the Sulawesi Sea of the Indonesian seas. The model simulation compares reasonably with the seasonal to interannual variability of the moored current meter observations in the upper 350 m or so of the Maluku Channel during 2015 and 2016. The interannual variability of the currents in the eastern Sulawesi Sea in the model is found to be associated with both the Pacific and Indian Ocean remote forcing. Lag correlation analysis and a theoretical linear wave model simulation suggest that both the equatorial Kelvin waves from the Indian Ocean and the coastally trapped Kelvin waves from the western Pacific along the Philippine coast can propagate through the Indonesian seas and arrive at the Maluku Channel. In particular, from mid-2015 to 2016 the Indian Ocean Kelvin waves are found to significantly impact the sea level anomaly variability in the Maluku Channel. The results indicate the importance of Indo-Pacific planetary waves to the interannual variability of the currents in the Sulawesi Sea at the entrance of the Indonesian seas.

Plain Language Summary The Indonesian seas provide a tropical connection for the climate systems over the tropical Pacific and Indian Oceans, the dynamics of which are not clear so far. This study uses a high-resolution computer model to simulate the currents measured by an acoustic current meter attached to a deep ocean mooring in the Maluku Channel of the northeastern Indonesian seas. Based on the successful simulation, the dynamics of the interannual variations of the circulation in the Maluku Channel are studied using the model and a simplified theoretical linear model. The interannual currents and sea level variability in the Maluku Channel are found to be affected by both the Indian Ocean Kelvin waves and the Philippine coastal Kelvin waves. It is found that the Indian Ocean Kelvin waves dominate the sea level variability in the Maluku Channel from mid-2015 to 2016. In early 2015, the sea level variability in the Maluku Channel is dominated by the coastal Kelvin waves from the east Philippine coasts. The results are important for the understanding of the circulation at the entrance of the Indonesian seas and of the Indo-Pacific interactions through the propagation of the planetary waves.

Key Points:
- Current observations from a mooring in the Maluku Channel within the Indonesian seas are reproduced well by the INDESO high-resolution model
- Interannual SLA variability in the Maluku Channel is affected by both Indian Ocean and Philippine coastal Kelvin waves
- SLA variability in the Maluku Channel is primarily forced by Indian Ocean Kelvin wave activity during 2015-2016

Supporting Information:
- Supporting Information S1

Correspondence to:
D. Yuan
dyuan@qdio.ac.cn

Citation:
Hu, X., Sprintall, J., Yuan, D., Tranchant, B., Gaspar, P., Koch-Larrouy, A., et al. (2019). Interannual variability of the Sulawesi Sea circulation forced by Indo-Pacific planetary waves. *Journal of Geophysical Research: Oceans*, *124*, 1616–1633. https://doi.org/10.1029/2018JC014356

Received 11 JUL 2018
Accepted 15 FEB 2019
Accepted article online 18 FEB 2019
Published online 10 MAR 2019

1. Introduction

The Indonesian seas represent a unique low-latitude connection between the tropical Pacific and Indian Oceans (Figure 1a). The ocean current flowing through this region, the Indonesian Throughflow (ITF), transfers warm, fresh surface water and cool, fresh thermocline water from the Pacific Ocean to the Indian Ocean, affecting the heat and salinity budget of both oceans (Godfrey, 1996; Gordon, 2005; Schneider, 1998; Sprintall et al., 2014). As the upper branch of the thermohaline circulation (Gordon, 1986), the ITF is also very important to the air-sea interaction and impacts and reacts to large-scale climate variability like the El Niño–Southern Oscillation (ENSO), the Indian Ocean Dipole, and the associated Asian monsoon variabilities.

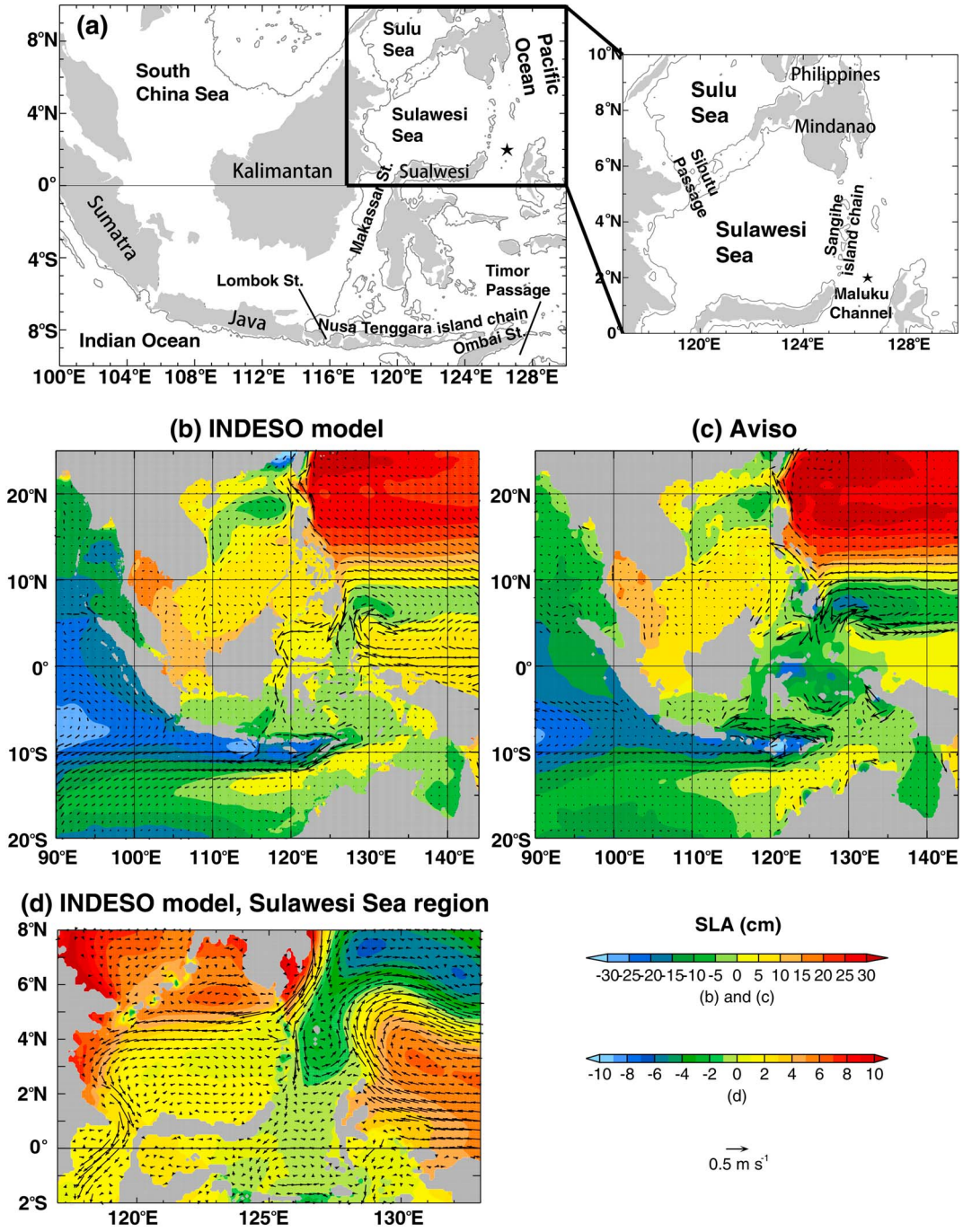

Figure 1. (a) Map of the Indonesian archipelago with names of the main islands and straits described in this paper; (b) sea surface height anomalies (cm) and surface currents (m/s) simulated by the INDESO model; (c) SLA and geostrophic currents from the Aviso altimetry product in the area of the model domain averaged over the 9 years from 2008 to 2016; and (d) is an enlarged portion of (b) in and around the Sulawesi Sea for detail. The light gray contours in (a) indicate the 200-m isobath based on National Oceanic and Atmospheric Administration's ETOPO2 data set. The mooring location in the Maluku Channel is marked by the black star in (a).

The Indonesian seas provide a crossroad for planetary wave activity from the Pacific and Indian Oceans (Wijffels & Meyers, 2004). In addition to the high-frequency intraseasonal oscillations including the Madden-Julian Oscillation, the variability in the equatorial Pacific Ocean between 5°N and 5°S is dominated by the annual Rossby waves generated in the middle of the year by the equatorial interior zonal wind field (Kessler & McCreary, 1993; Kessler & McPhaden, 1995; Yuan, 2005) and the interannual Rossby waves forced by the interannual zonal winds (Boulanger & Menkes, 2001; Yuan et al., 2004). Kessler and McPhaden (1995) demonstrate that it takes several months for the annual Rossby waves to propagate from the mid-Pacific Ocean basin to the western boundary. Traditional linear equatorial wave dynamics suggest that one third of the first mode Rossby wave energy reflects back into the Pacific as the equatorial Kelvin waves at the entrance of the Sulawesi Sea (Clarke, 1991; Du Penhoat & Cane, 1991). Using a numerical model, Spall and Pedlosky (2005) show that 23% of the energy from the equatorial Rossby wave is reflected into the Kelvin wave at the leaky western boundary of the Pacific Ocean with only 10% of the energy reaching the Indian Ocean. Recent studies find that the western boundary reflections are nonlinear (Yuan, 2005; Yuan et al., 2004). The nonlinear reflection is associated with the shifting of the Mindanao Current path (Yuan, Li, et al., 2018). In the off-equatorial Pacific Ocean, Rossby waves propagate westward and impinge on the coast of Mindanao, and some of that Rossby wave energy can reflect as eastward propagating equatorial coupled waves (White et al., 2003). The remainder can propagate along the coast of the Philippines as coastally trapped Kelvin waves and penetrate into the South China Sea through the Sulawesi Sea and the Sulu Sea (Q. Liu et al., 2011) and potentially into the Indian Ocean (McClean et al., 2005).

In the Indian Ocean, the Kelvin waves generated by the equatorial Indian Ocean wind reversals propagate eastward along the equatorial waveguide. Previous observations (Meyers, 1996; Sprintall et al., 2009; Wyrtki, 1987) and simulations (H. Liu et al., 2005; Murtugudde et al., 1998) indicate that the intraseasonal (Arief & Murray, 1996; Drushka et al., 2010; Qiu et al., 1999; Syamsudin et al., 2004), semiannual (Sprintall et al., 2000; Sprintall et al., 2009; Susanto et al., 2012), annual (Potemra, 1999), and interannual (Yuan, Hu, et al., 2018; Yuan et al., 2011, 2013) Indian Ocean Kelvin waves can impact the ITF properties and transports when propagating into the Indonesian seas. The Kelvin waves from the Indian Ocean can influence currents at the Lombok Strait through coastally trapped Kelvin waves (Drushka et al., 2010; Qiu et al., 1999; Sprintall et al., 2000; Syamsudin et al., 2004). To satisfy the geostrophic balance in the direction perpendicular to the coast, these coastal Kelvin waves can only propagate southeastward along the Sumatra-Java coasts and so keep the coast on their left (in the Southern Hemisphere). The Kelvin waves can also propagate into the Indonesian seas from Lombok Strait to Makassar Strait as the second and third baroclinic modes (Pujiana et al., 2013, 2009). Yuan, Hu, et al. (2018) show that these Kelvin waves can continue to propagate further north through the Sulawesi Sea and arrive at the Maluku Channel in a theoretical model. To our knowledge, no studies have as yet determined how much contribution these waves make to the interannual variability of the sea level at the Maluku Channel in the Sulawesi Sea and how they might interact there with the incoming planetary wave energy from the Pacific Ocean.

In this study, we focus on the fate of these planetary waves from both the Pacific and Indian Oceans in the Sulawesi Sea using a high-resolution regional ocean model and a linear model. Altimeter data and mooring observations in the Maluku Channel will be used to validate the model and investigate the wave propagation. Data sets and models are introduced in section 2. Main results are shown in section 3, followed by discussions and conclusions in section 4.

2. Data and Models

2.1. Observed Data

2.1.1. Moored Measurements

Three moorings were deployed in the west, central, and east Maluku Channel from November 2014 to November 2016 during the joint cruises between Institute of Oceanology of the Chinese Academy of Sciences and Research Center for Oceanography of the Indonesian Academy of Sciences (RCO/LIPI), which fully covered the strong El Niño event started in early 2015. In this paper, we only focus on the middle mooring located in the central Maluku Channel (2°N, 126.48°E, black star in Figure 1a) since it appears that the other two moorings were subject to localized circulation patterns associated with side wall boundaries. A 75-KHz upward looking acoustic Doppler current profiler (ADCP) measuring the vertical profile of horizontal currents was mounted at a nominal depth of 450 m. The vertical bin size and the time interval of the ADCP sampling are 8 m and 1 hr, respectively. Surface measurements in the upper 0–35 m are missing

because the ADCP is either too deep to reach the surface or is subject to contamination from surface reflection. The velocities of the ADCP are interpolated onto a 5-m vertical grid between 35 and 400 m. A few bins with missing values were filled with linear interpolation.

2.1.2. Remotely Sensed Data

The Aviso gridded sea level anomaly (SLA) product is used to validate the model and investigate the wave propagation. This product is merged from different altimeter measurements: HY-2A, Jason-2, Topex/POSEIDON, ENVISAT, ERS-1/2, and so on. An ocean tide model FES2014 has been used to correct the data and the residual noise is filtered out (CLS, 2016). The data cover the global ocean on a 0.25° by 0.25° grid from January 1993 to May 2017. We use the daily mean product made available by Aviso from the near weekly satellite data, which is the same time interval as the model output.

2.1.3. Ancillary Data

Daily mean European Centre for Medium-Range Weather Forecasts (ECMWF) ERA-Interim surface winds on a 0.5° longitude by 0.5° latitude grid are used to calculate the wind stress and also to force the linear Kelvin wave model (sections 2.2.2, 3, and 4).

The Oceanic Niño Index (ONI) used in this paper is from the National Oceanic and Atmospheric Administration Climate Prediction Center. This monthly index is calculated from a 3-month running mean of the sea surface temperature anomalies in the Niño 3.4 region (5°N–5°S, 120–170°W) using the National Oceanic and Atmospheric Administration ERSST Version 4, from 1950 up to 2017.

2.2. Models

2.2.1. INDESO

The high-resolution simulation output used in this paper is from the NEMO ocean model (http://www.nemo-ocean.eu). The model allows for a variety of configurations, and here we use the one regionalized in the Indonesian seas developed as part of the INDESO project, hereinafter referred to as the INDESO model. In this model, the tides are explicitly resolved and forced by a tidal forcing at boundaries. An additional parameterization is also used to improve the tidal mixing induced by the internal waves (Koch-Larrouy et al., 2007). The model has a horizontal resolution of 1/12° and 50 vertical layers from the sea surface (0.5 m) to 5,727.9 m with a depth-dependent resolution that has 26 layers above 200 m, 9 layers between 200 and 1,000 m, and 15 layers below 1,000 m. The model covers the area from 20°S to 25°N and from 90°E to 144°E, which includes the entire Indonesian seas (Figure 1). It was forced by the 3-hourly ECMWF atmospheric fields from 2008 to 2016. Open boundary conditions are located on a relaxation band of 10 grid points (~1°) and come from daily output of the Global Ocean Forecasting System at 0.25° forced by 3-hourly ECMWF operational forcings, offered by the Mercator Océan Service. More detailed description of the model can be found in Tranchant et al. (2016) and Nugroho et al. (2017).

2.2.2. The Linear Coastally Trapped Kelvin Wave Model

Sprintall et al. (2000) used an analytical linear Kelvin wave model (Gill, 1982) to predict the Indian Ocean Kelvin wave propagation into the Lombok Strait forced by winds in different sections along the Kelvin wave pathway. Here we extend the solution in the Indonesian seas based on the Gill (1982) model. The model integrates the zonal momentum equation in the alongshore direction in the form:

$$\frac{\mathrm{d}A_k}{\mathrm{d}t} + c\frac{\mathrm{d}A_k}{\mathrm{d}x} = \frac{cX}{g} \tag{1}$$

where A_k denotes SLA along the Kelvin wave characteristics, X is the alongshore wind stress projected onto each baroclinic mode using the vertical modes from the INDESO model above, and c is the wave speed of the model baroclinic modes, set to be 2.71 m/s for the first baroclinic mode. In equation (1), we substitute for x using $t = x/c$, so the integration of (1) along the Kelvin wave characteristics gives the solution of A_k at any location along a Kelvin wave pathway at any time.

3. Results

3.1. INDESO Model Evaluation

Tranchant et al. (2016) provide a reasonably comprehensive evaluation of the INDESO model mean circulation, sea surface salinity, tides, ITF transport, and so forth using existing observational data sets. However, the model circulation at the ITF entrance has not been validated. Here we evaluate the model using observations of satellite SLA and the mooring data from the Maluku Channel that bounds the Sulawesi Sea (Figure 1).

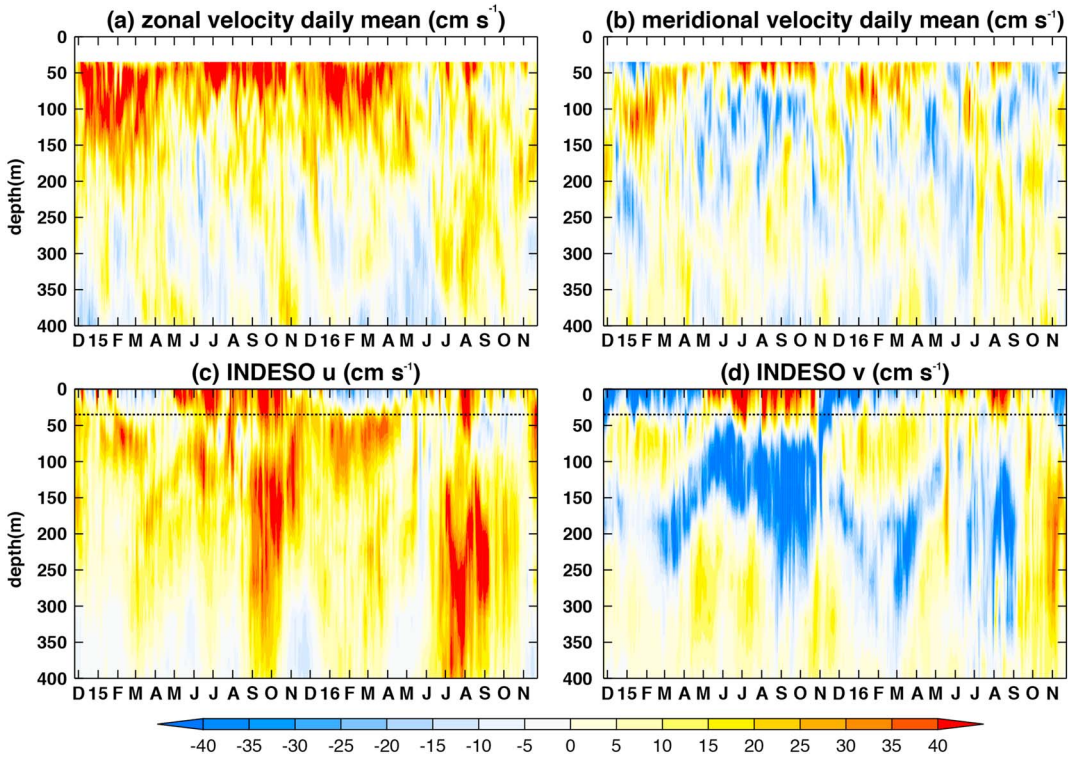

Figure 2. Zonal and meridional currents (cm/s) over the upper 400 m from the Maluku Channel mooring (a, b) and the INDESO model (c, d) from November 2014 to November 2016. The model currents are averaged in a 1/6° × 1/6° box centered at the mooring location at 2°N, 126.48°E. The dotted lines in (c) and (d) indicate the shallowest depth (35 m) of the corresponding mooring data.

The model and observed SLA over the same 9-year period (2008–2016) are found to share the same patterns, including the overall SLA gradient from the (lower) Indian Ocean to the (higher) Pacific Ocean, and the positive (negative) SLA center associated with the anticyclonic (cyclonic) circulation in the subtropical and tropical Pacific Ocean (Figures 1b and 1c). Within the Indonesian Archipelago there exist some subtle differences. The model 9-year mean SLA has positive anomalies in the northern Makassar Strait, Sulawesi Sea, Sulu Sea, northeast of Sulawesi (near Mindanao Island), Halmahera Sea, and the southwestern coast of the western New Guinea, but the SLA of this area is negative in the observations. These differences may be a result of tides, which have significant amplitudes in the coastal regions. The INDESO model explicitly includes the baroclinic and barotropic tides, while the altimeter SLA is corrected using a barotropic tide model. Tranchant et al. (2016) show that the model has very good agreement with regional tide gauge observations for periods longer than 10 days. Alternatively, the coarse resolution of the altimeter data compared to the model could be another reason for some of the discrepancy in SLA.

The mean surface currents of the model and the geostrophic currents from the altimeter data are also presented in Figure 1b/1d and Figure 1c, respectively. Due to the small Coriolis force, the geostrophic currents near the equator (4°S to 4°N) are not calculated using the altimeter data. The model currents show the expected general circulation of the Indo-Pacific Ocean (Figure 1b), as do the geostrophic currents (Figure 1c). The mean North Equatorial Current (NEC), North Equatorial Counter Current, and South Equatorial Current in the Pacific Ocean are evident. The NEC splits into the Kuroshio and the Mindanao Currents at the latitude of about 12.5°N, which is slightly equatorward of the climatological mean of the NEC bifurcation latitude of 15.5°N (Hu et al., 2015). In the Indian Ocean, the South Java Current along the Java coast and the westward South Equatorial Current at about 12°S are prominent features of the mean flow. In the Indonesian seas, the ITF from the Pacific Ocean to the Indian Ocean through the Makassar Strait in the model is stronger than that through the eastern inflow passages, consistent with the perspective that the Makassar Strait is the primary ITF inflow pathway (Gordon et al., 2010).

The upper-ocean currents in the Maluku Channel have been rarely observed in history. Luick and Cresswell (2001) only obtained valid observations of the currents below 740 m using current meters. Ship-board ADCP observations by Kashino et al. (2001) were obtained in the northern Maluku Sea, but the single transect of velocity data was inevitably aliased by tides and internal waves that are strong in the area. Here we take advantage of the recent moored ADCP observations in the Maluku Channel (Yuan, Li, et al., 2018) to assess the model's skills in reproducing the zonal and meridional currents from the mooring observations at 2°N, 126.48°E (Figure 2). The model currents are averaged in a 1/6° × 1/6° box surrounding the mooring location. For the zonal velocity, the mooring observation (Figure 2a) and the INDESO model (Figure 2c) agree fairly well with each other above 150 m being mainly eastward except for the boreal summer and fall seasons of 2016. The model successfully simulated the significant eastward currents at the beginning of both 2015 and 2016 (January to April), albeit with slightly smaller amplitude. From 150 to 400 m, although the zonal currents of the model and observation share the same pattern of eastward flow during boreal fall, the INDESO current is much stronger. In addition, westward flow observed from June to July 2015 between 150 and 300 m and at the beginning of 2016 centered at 300-m depth is not successfully simulated by the model.

The patterns of the meridional currents in the observation (Figure 2b) and the model (Figure 2d) are quite similar over the available depth range with an obvious annual variability. Both show northward currents during the boreal winter-spring seasons of each year at 50 to 120 m. Maximum velocities in the model are deeper in 2016 and shallower in 2015 compared to the observations. Southward flow from May to October 2015 at ~150 m is also correctly simulated except the amplitude is twice as large in the model compared to the observations. Current speeds are also overestimated at the end of 2016, when the northward flow is much stronger in the model than in the mooring observations below 150 m.

To investigate the seasonal cycle of the currents in the Maluku Channel, we have extracted the annual and semiannual harmonics from the observations (Figures 3c and 3d) and compare them with those from the model over the same period as the observations (Figures 3e and 3f) and for the full 9-year model record (Figures 3g and 3h), respectively. The annual regional monsoon wind in this northern part of the Indonesian seas averaged in the region (1–3°N, 125–128°E) is dominated by the meridional wind forcing, which appears northward from June to October and southward during the remainder of the year (Figures 3a and 3b). Both the zonal and meridional currents in the Maluku Channel show an annual variability in the upper layer above 150 m, while the semiannual signal dominates below (Figures 3c–3h). Comparison between model and observation in the upper layer between 35 and 150 m is quite good, except that the model results are a little weaker than the observation. In this layer, northeastward flow appears during boreal winter-spring and southwestward flow exists in summer and fall, with cores at 75 m for zonal current and 100 m for meridional current in both observation and model (Figures 3c–3f). This directional flow corresponds to the annual changes in the meridional wind stress (Figures 3a and 3b). In the subsurface below 150 m, the variability can be described as semiannually alternating northeastward and southwestward flows. The separation depth that distinguishes the annual/semiannual variability is shallower in the model of the full 9-year record (~120 m) compared to the observation (~180 m) and the model simulations over the same period as the observation (~200 m). This is probably due to the contamination of the seasonal cycle of the thermocline depth by the interannual variations in the observational period, since the differences between the seasonal cycle of the temperature profiles over the entire 9-year time series and during the same period as the moored observations concentrate between 150 and 200 m (not shown). The lower layer is dominated by semiannual variability, with the eastward velocity at ~250 m in boreal fall much stronger in the model than in the observation (Figure 3e). The biggest difference in the meridional velocity is that the model semiannual signal lags the observation by about 2 months (Figures 3d, 3f, and 3h), which implies that the model may not simulate the circulation patterns below 150 m very well. The amplitude of the entire seasonal variability is also much larger in the model than in the observation.

To have a quantitative understanding of how much the model can express the real current, we also present the percent variance explained by the model in the observed currents (Figure 4). In the upper layer, dominated by annual variability above 120 m for the zonal velocity and 180 m for the meridional velocity (e.g., Figures 3e and 3f), the INDESO model of both the observational period and the entire time series explains over 80% of the observation variability. Below these depths, the percent variance explained by the entire model time series is only half of that explained over the same period of the observations (60–80%). The mini-

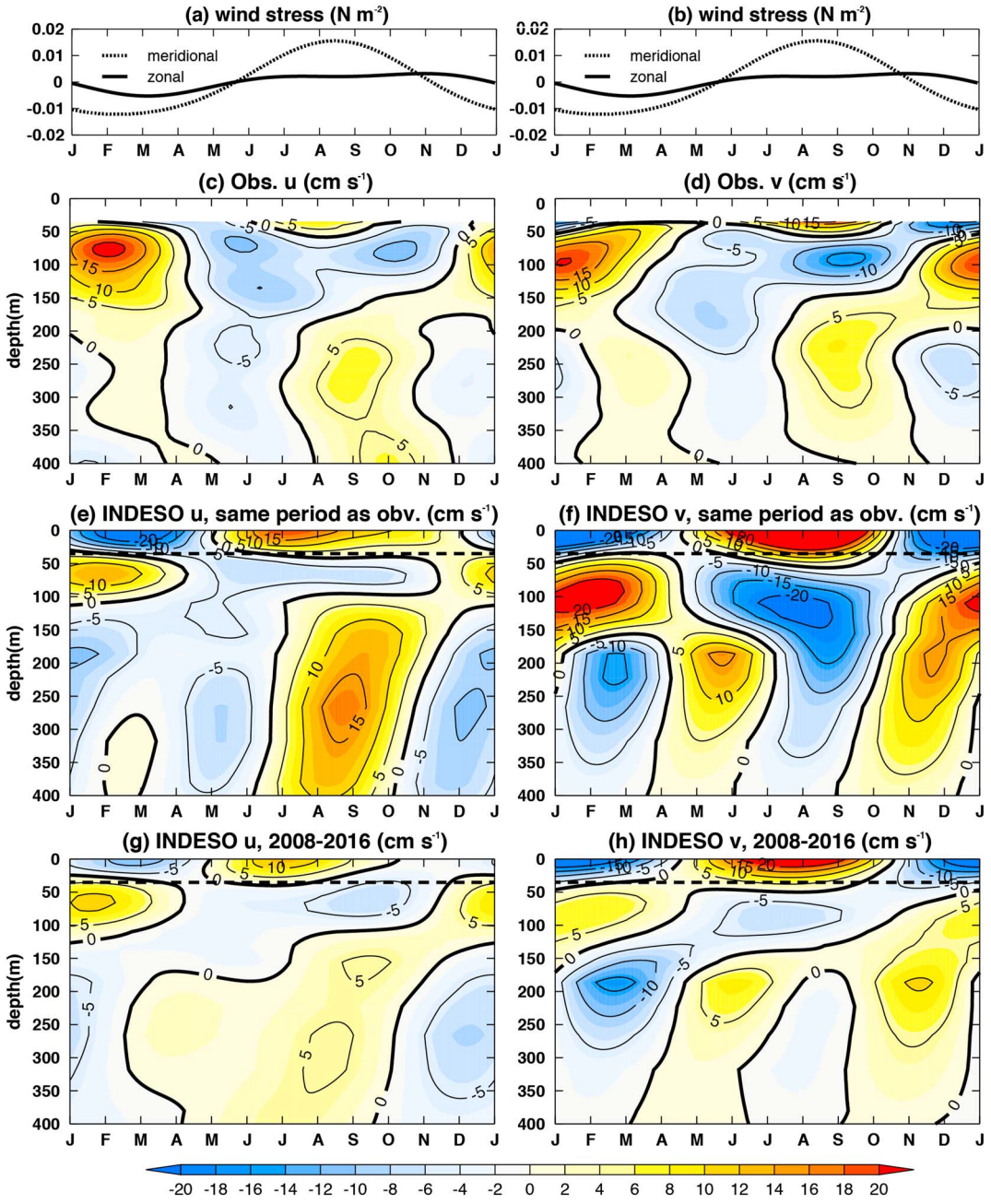

Figure 3. Seasonal zonal and meridional wind stress (N/m^2, a, b) averaged between 1–3°N, 125–128°E and observed (c) zonal and (d) meridional currents (cm/s) over the upper 400 m from the Maluku Channel mooring, and the corresponding INDESO model seasonal zonal and meridional currents over the same period as the observations (e, f) and for the full 9-year record (g, h). The dash lines in (e)–(h) indicate the shallowest depth (35 m) of the corresponding mooring data.

mum of the explained variance between 150 and 200 m is because of the difference in the depth of the upper layer that separates the annual/semiannual variability in the model and observations as discussed above.

The time-averaged zonal velocity profile over the mooring observation period at both the mooring and in the INDESO model are eastward (Figure 5a). In the INDESO model, the zonal velocities and their standard deviation are fairly constant above 280 m, with a mean of ~15 cm/s and standard deviation of ~10 cm/s. In contrast, the observations show a maximum zonal velocity at 50 m of ~30 cm/s. The standard deviation

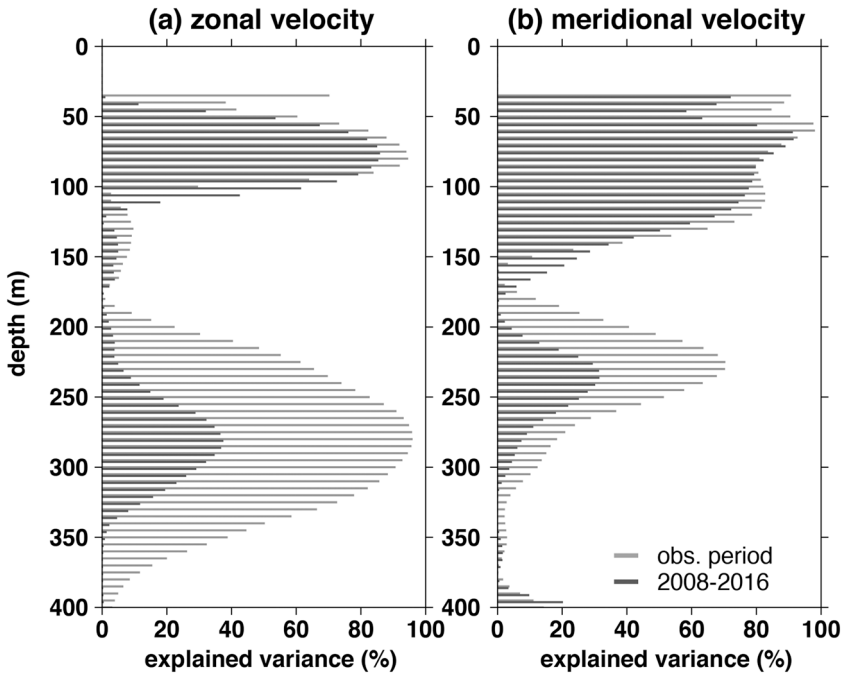

Figure 4. Percent variance explained by the INDESO model of the mooring observation period (light gray) and the period of 2008–2016 (dark gray) in seasonal (a) zonal and (b) meridional velocity over the upper 400 m at the Maluku Channel.

at the surface in the observations is also larger than the model results. The observed mean zonal velocity decreases rapidly from 50 to 200 m, from about 30 to less than 5 cm/s.

For the mean meridional velocities, the model results show the same pattern as in the observations: northward flow at depths above 60 m, southward flow in the subsurface layer (60–270 m), and weak but northward flow in the deeper layer below 270 m (Figure 5b). In the upper layer the maximum observed velocity (~8 cm/s) is much stronger than that of the model (~3 cm/s) but occurs at the same depth of about 45 m. Between 70 and 250 m the mean meridional flow in the model is strongly southward (~15 cm/s), although quite variable, while the mean meridional velocity in the observations is near 0. This difference could originate from the model anomalies during a strong El Niño state—specifically, the model velocity is more strongly southward than observations during May–October 2015 (Figures 2b and 2d). Below 270 m, both the model and observations show very weak flow.

In general, compared with the mooring observations, the patterns of the current variability with depth above 150 m are simulated quite well by the model particularly over seasonal time scales. In the lower layer between 150 and 400 m, the simulated meridional velocity overestimates the observations with a phase shift in the semiannual cycle.

3.2. Interannual Variability of the Circulation at the Maluku Channel

Considering the relatively favorable comparisons with the Maluku Channel mooring observations above 150 m and the Aviso SLA noted above, and other environmental parameters (Tranchant et al., 2016), the INDESO model is used to investigate the interannual variability of the circulation in the Indonesian seas over the entire 9-year time period from 2008 to 2016. After removing the 9-year climatological mean of each day from the time series we obtain the interannual variability of the regional wind stress averaged from 1°N to 3°N and from 125°E to 128°E and velocities at the Maluku Channel (Figure 6). A 120-day fourth-order Butterworth low-pass filter is applied to filter the interannual anomalies of the wind stress and the velocities. The positive and negative values represent the southerly and northerly anomalies, respectively.

During the boreal winters of the years 2009–2010, 2014–2015, and the second half of 2015, the flow is anomalously southward and eastward above 200 m (Figures 6b and 6c, green boxes), although the strength of the anomalies scales with the strength of the El Niño (Figure 6a, ONI), corresponding to the southerly wind stress anomalies, which are a little ahead of the positive peaks of the ONI (Figure 6a). For example,

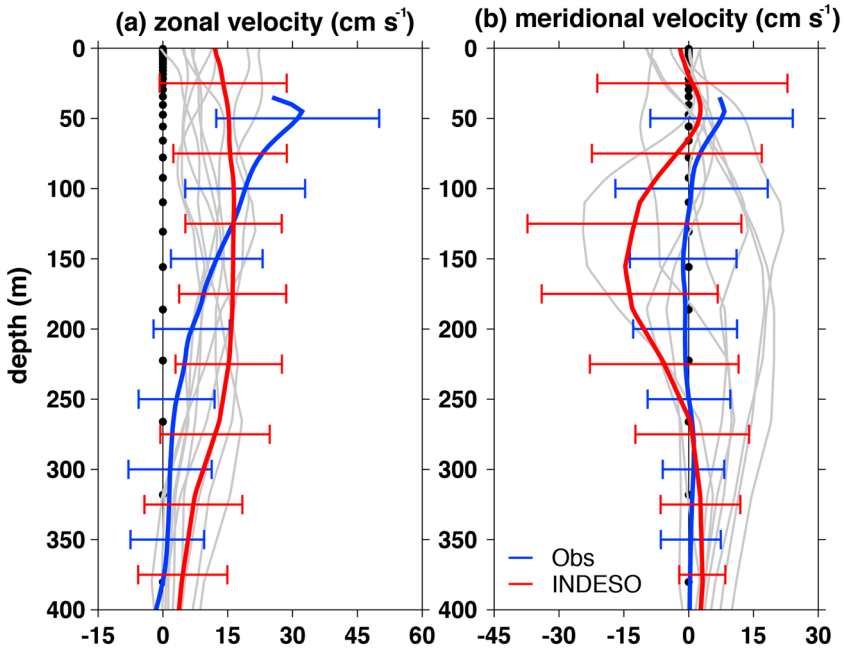

Figure 5. Time-averaged (a) zonal and (b) meridional velocities (cm/s) from the surface to 400-m depth for the Maluku Channel observations (blue curves) and the INDESO model (red curves) of the same observational period. The bars show the standard deviations. Thin gray curves represent the annual mean of INDESO model velocities of each year from 2008 to 2016. Black dots along the zero grid lines are the vertical layers of the INDESO model.

2015–2016 is a relatively strong El Niño compared to 2009–2010, and the current anomalies are much larger and lasted longer in 2015–2016 than in 2010, as did the wind stress. It is worth mentioning that these two El Niño events are different not only in strength but also in patterns. The extreme 2015–2016 event is a mixture of the central Pacific and east Pacific El Niños (Paek et al., 2017). In contrast, the 2009–2010 El Niño is an event of the central Pacific type (Yu et al., 2012). The Walker circulation variations during these two events are different. The behaviors of the current responding to the wind stress variations are also different: The southeastward current anomalies appear before the peak of the ONI during the 2015–2016 event, whereas they are coincident with the peak of the ONI during the 2009–2010 event. However, the current anomalies in the Maluku Channel during both events are to the southeast, suggesting a similar relationship to the basin-scale forcing associated with either ENSO events.

An empirical orthogonal function (EOF) analysis is applied to the interannual anomalies of the SLA and currents averaged between 55 and 180 m in the northeastern Indonesian seas. Here we limit our attention to the leading EOF mode of the interannual variabilities (Figure 7), which accounts for 89.4% of the SLA and 32.9% of the velocity variances, respectively. The corresponding principal components of the SLA and velocity show relatively high correlation (0.885 for SLA and 0.756 for velocity) with the Niño index (Figures 7a and 7b), indicating that this mode is related to ENSO dynamics. The spatial mode shows strong currents in the Maluku Channel and at the entrance of Sulawesi Sea, while the currents in the western part of the Indonesian seas, such as in the Makassar Strait, are weak. This indicates that the interannual variabilities of the currents at the entrance of the Sulawesi Sea and the western boundary of the Pacific Ocean are much stronger than those of the currents in the western passages (the Makassar Strait). As such, there is a significant connection between the circulation at the entrance of Sulawesi Sea and the western boundary currents over interannual time scales. The pattern shows that during the El Niño years, the Mindanao Current joins the Mindanao Eddy-Halmahera Eddy retroflection directly at 2.5°N, together with the northward currents from the western Maluku Channel. In this situation, currents at the central Maluku Channel appear southeastward (Figure 7c). At the same time, the Makassar Strait throughflow has positive anomalies, which is in accordance with previous observations of a weak and northward along strait velocities at the surface during El Niño (Gordon et al., 2012; Susanto et al., 2012). In contrast, during the more typical years, the currents in the west of the Maluku Channel turn to be southward, intruding into the Maluku Channel to 1°S then turning northward to exit in the eastern Maluku Channel and join the North Equatorial Counter Current via

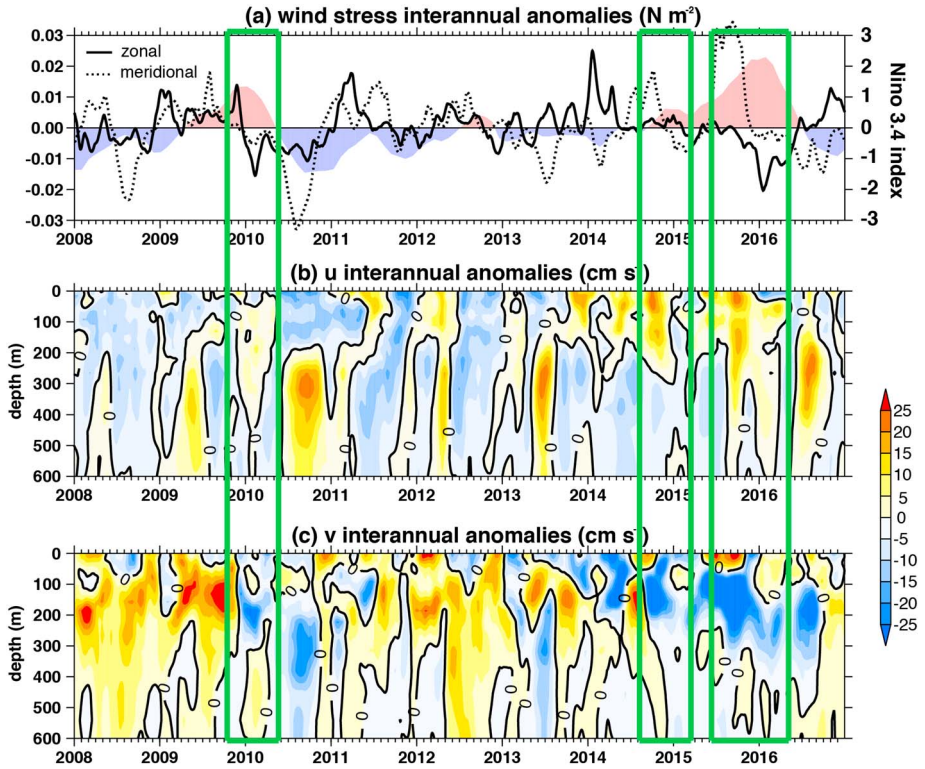

Figure 6. (a) Interannual daily zonal and meridional wind stress anomalies averaged in the region 1–3°N, 125–128°E (solid and dash curves, N/m^2) with monthly Niño index (red and blue shadings, °C). (b) Interannual zonal and (c) meridional anomalous currents (cm/s) at the location of the central Maluku mooring site from the INDESO model during 2008–2016. Green boxes mark three periods of the current anomalies.

the Halmahera Eddy. These flows form a recirculation pattern in the Maluku Channel and produce weak currents in the central Maluku Channel (Figure 1d). This phenomenon suggests that the variation of the currents at the central Maluku and at the entrance of the Sulawesi Sea may be influenced by some dynamical processes related to ENSO associated variability, like oceanic planetary waves.

3.3. Role of the Oceanic Waves

In this section, an analytical linear Kelvin wave model is used to study the wave propagation from both the Indian and the Pacific Oceans through the Sulawesi Sea. We performed the correlation between the observed

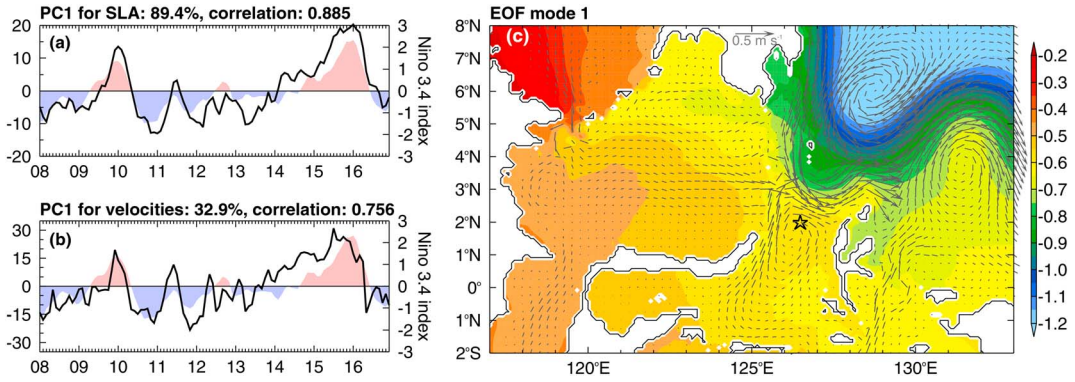

Figure 7. Principal components of the interannual anomalies of the (a) sea level anomaly and (b) velocity and (c) spatial patterns of the first empirical orthogonal function mode. The velocity overlain on (c) is averaged between 55 and 180 m. The red and blue shadings in (a) and (b) mark the El Niño and La Niña events, respectively, from the monthly Niño index (°C). The black star in (c) indicates the location of the Maluku Channel mooring.
EOF = empirical orthogonal function; SLA = sea level anomaly.

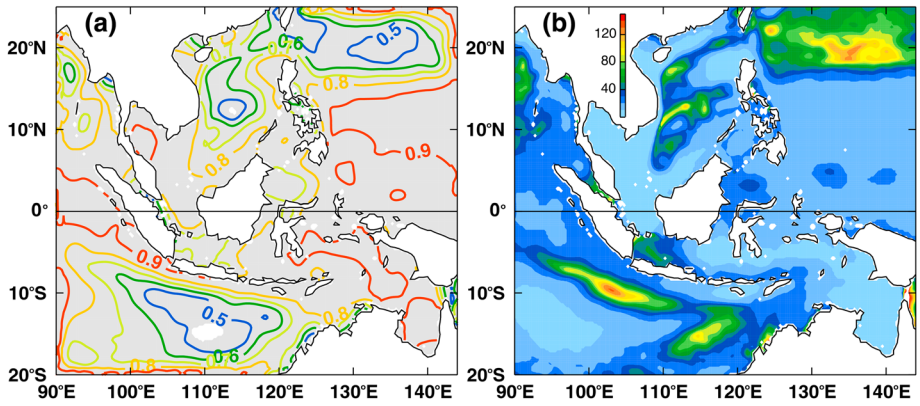

Figure 8. (a) Correlations between the SLA simulated by the INDESO model and from the Aviso altimetry product over the 9 years from 2008 to 2016. Gray shading in (a) indicates correlations significant above the 95% confidence level, based on the effective number of degrees of freedom in (b). The effective number of degrees of freedom is calculated following the equations described by Emery and Thomson (2001).

and model simulated SLA across the whole model domain (Figure 8). The correlation is significant above 95% level in most of the Indonesian seas between 10°S and 10°N, which shows the good skill of the model in simulating the variation of the SLA in this region. On this basis, SLA variability from the model is used to identify the waveguide.

3.3.1. Indian Ocean Kelvin Waves

As noted above, Kelvin waves from the Indian Ocean can potentially propagate through the Indonesian seas and influence the circulation within the Sulawesi Sea (Yuan, Hu, et al., 2018). Here we determine a waveguide pathway from the Indian Ocean to the Maluku Channel and calculate the lag correlations of the SLA between successive points along the pathway and the Maluku Channel (Figure 9a) using observed Aviso data (Figure 9b) and INDESO simulations (Figure 9c). Positive days in the lag correlations indicate the SLA at that location leads that in the central Maluku Channel. There is a significantly high correlation (above 0.5) found all the way from the eastern Indian Ocean to the Maluku Channel. The highest correlation occurs at lags of 0 to 18 days. The slope of the highest correlations in space and with time lag is roughly consistent with the Kelvin wave speed of the first baroclinic mode (black solid lines in Figures 9b and 9c) from the eastern Indian Ocean to the Maluku Channel. The INDESO simulation does not resolve the first baroclinic mode wave propagation as well as the Aviso data, probably due to errors of the atmospheric forcing that produce the artificially high correlations at the zero time lag. There is also agreement between the slope of the high correlation and the Kelvin wave speed of the second and third baroclinic modes from the Lombok Strait to the Maluku Channel (black dashed and dotted lines in Figures 9b and 9c). This indicates a propagation of the Kelvin wave with a speed of the theoretical second and third baroclinic mode Kelvin waves through the Makassar Strait, which is consistent with the observation of Pujiana et al. (2013). The correlations in the model are higher than in the observations, probably because the Aviso product is too coarse to resolve some coastal processes in the Indonesian seas. Thus, the strong correlations suggest that the signal at the Maluku Channel can be affected by the Kelvin waves from the Indian Ocean.

Sprintall et al. (2000) investigated the Kelvin wave propagation from the Indian Ocean to the Lombok Strait using a theoretical coastal Kelvin wave model (Gill, 1982). Here we extend the model through the Makassar Strait to the Maluku Channel to provide a more quantitative assessment of the Kelvin wave propagating through the Indonesian seas. The model was integrated in two parts: (1) from the Indian Ocean to the Lombok Strait as the first baroclinic Kelvin wave mode (e.g., Sprintall et al., 2000) and (2) from the Lombok Strait to the Maluku Channel as the third baroclinic mode Kelvin waves with a speed of 1.0 m/s (e.g., Pujiana et al., 2013). No loss of energy associated with reflected Rossby waves or the northward propagating Kelvin wave along the west Sumatra coast is considered during the integration of the first part (Clarke, 1991; Sprintall et al., 2000). Theoretical studies demonstrate that the Lombok Strait is wide enough for nearly all of the incoming Kelvin wave energy to propagate through (Durland & Qiu, 2003). Drushka et al. (2010) quantified the amount of the intraseasonal Kelvin wave energy entering the Lombok Strait with observations and suggest that 37% ± 9% of the incoming Indian Ocean Kelvin wave energy bypasses the Lombok Strait and continues eastward. The remaining 60% enters the internal Indonesian seas via Lombok Strait or is dissi-

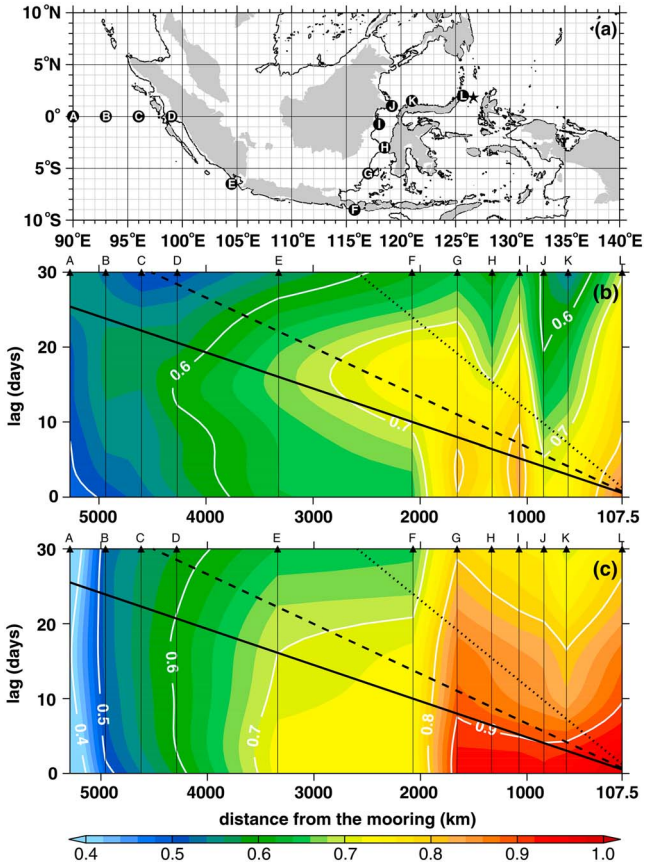

Figure 9. (a) Map of the potential Kelvin wave coastal waveguide pathway from the Indian Ocean (point A) through the Indonesian seas to the Maluku Channel mooring (black star). Black contours indicate the 100-m isobath. (b) Lag correlations of the Aviso altimeter data between points along the possible waveguide and at the mooring location in the central Maluku Channel. (c) Same as (b) but for INDESO SLA. Black solid, dashed, and dotted lines in (b) and (c) denote theoretical first to third baroclinic mode Kelvin wave phase speeds, respectively, for reference.

pated or reflected. The energy bypassing the Lombok Strait will propagate eastward, turn northward through the Ombai and the Timor Straits, and then propagate westward along the northern coastline of the eastern Nusa Tenggara island chain and arrive at the Lombok Strait again. It only takes several days for this process to occur. Since we mainly focus on the interannual time scales here, the phase shift between the incoming Kelvin wave directly propagating northward through the Lombok Strait and the waves coming back from the Ombai and the Timor Straits can be omitted. Hence, we start from 100% of the amplitude of SLA at the Lombok Strait when integrating the second pathway of the model through the Makassar Strait. A linear reduction of ~40% of the SLA amplitude near the equator is applied when integrating the second path after the Lombok Strait due to the change in the radius of deformation from an off-equator latitude to the equator (Yuan, Hu, et al., 2018).

The SLA in the central Maluku Channel is predicted using the Gill (1982) analytical model and compared with the observed Aviso SLA at the same location (Figure 10). The model integrates the wind stress projected in the alongshore direction along the Kelvin wave pathway starting from the Indian Ocean to the Maluku mooring site (Figure 9a). The agreement between the model and altimeter data at the beginning of 2015 is not very good, but the two SLA signals are very coherent after June 2015 (Figure 10a). The correlation coefficients between the simulated and observed SLA during the first half year of 2015 and the remainder of the time series are 0.17 (below the 95% significance level at 0.51) and 0.87 (above the 95% significance level at 0.75), respectively. The significance tests are based on the effective numbers of degrees of freedom (DOF) of 13 and 5 (Emery & Thomson, 2001). The model successfully predicts the peak from December 2015 to January 2016 and from June to August 2016, which suggests that the Indian Ocean Kelvin wave energy can affect the interannual variability at the Maluku Channel by propagating through the Indonesian seas. To

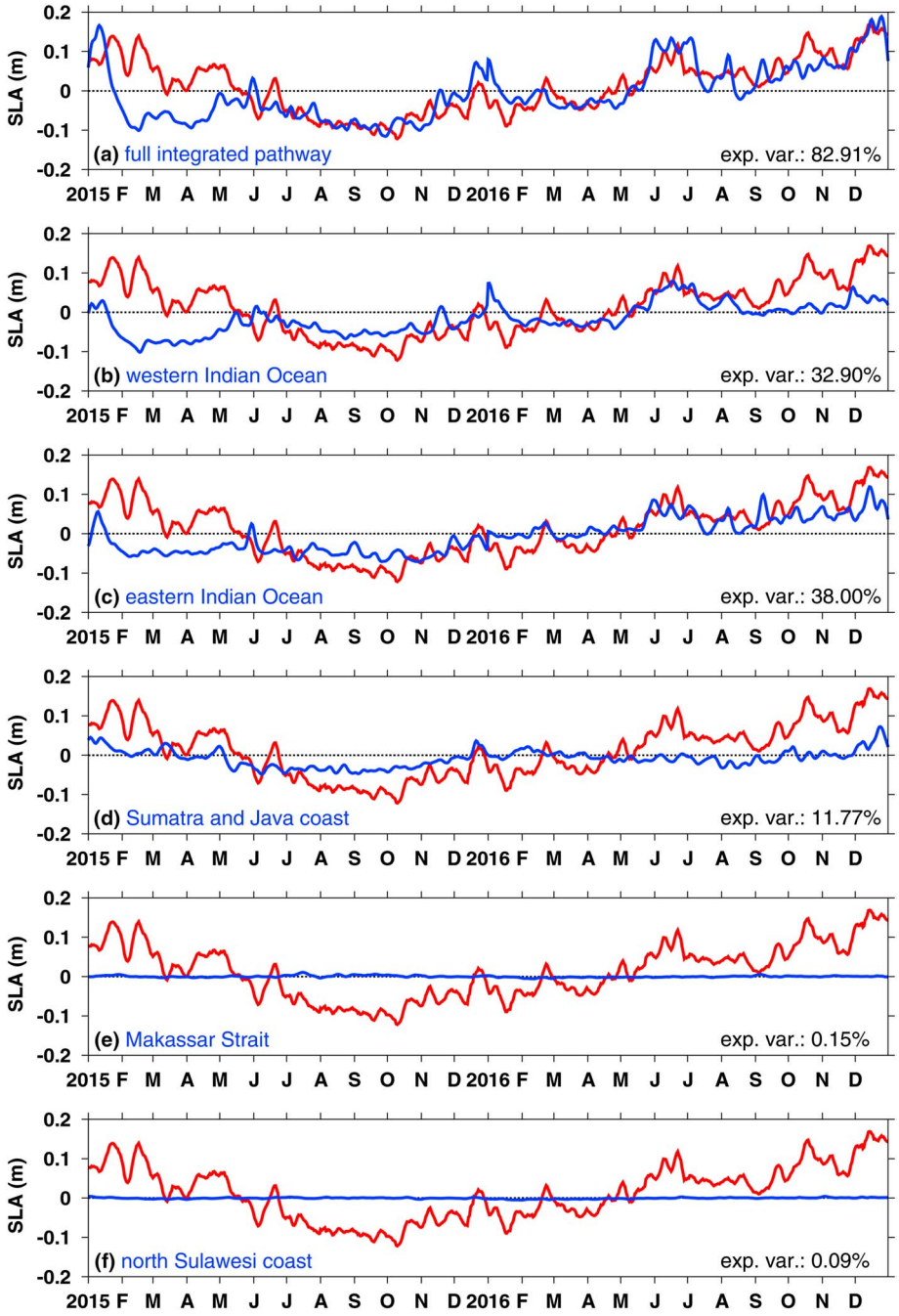

Figure 10. Comparison of the Aviso SLA at the central Maluku Channel (red curves) and SLA predicted from the Kelvin wave model (blue curves) integrated along the pathway from the western Indian Ocean (0°, 45°E) to the Maluku Channel (2°N, 126.5°E) forced by different wind stress sections: (a) the full pathway, (b) only in the equatorial western Indian Ocean from (0°, 45°E) to (0°, 75°E), (c) only in the equatorial eastern Indian Ocean from (0°, 75°E) to (0°, 99°E), (d) along the coast of Sumatra and Java from (0°, 99°E) to (9°S, 115.5°E), (e) along the 100-m isobath in the Makassar Strait from (9°S, 115.5°E) to (1°N, 120°E), and (f) along the coast of north Sulawesi from (1°N, 120°E) to the Maluku Channel (2°N, 126.5°E). SLA = sea level anomaly.

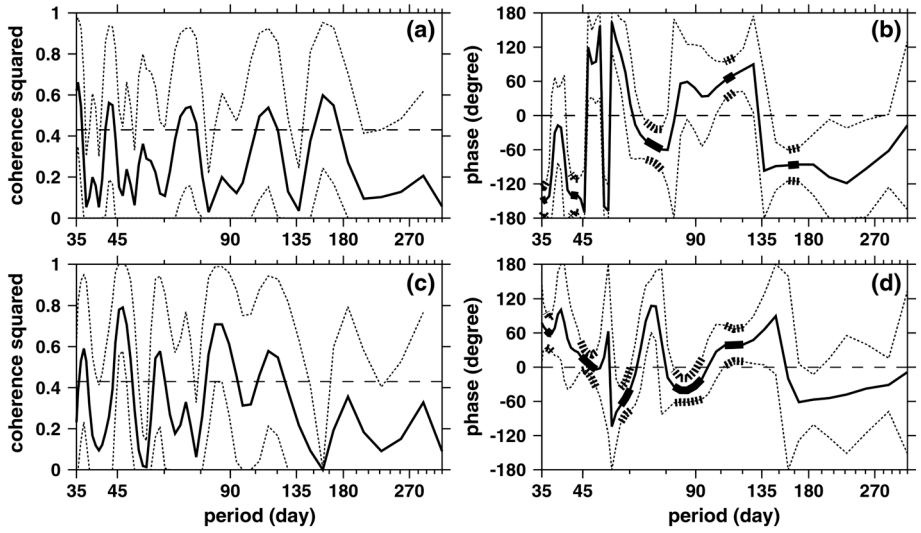

Figure 11. Coherence-squared and phase functions between the sea level anomaly near the Philippines at (7.5°N, 126.75°E) and that in the central Maluku Channel at the mooring location at 2°N, 126.48°E calculated using the (a, b) Aviso altimeter data and (c, d) INDESO model. The 95% confidence intervals are plotted in dotted lines in (a) and (c). The dashed lines in (a) and (c) indicates the 95% significant level of the coherency-squared function. The bold lines in (b) and (d) represent the phase function where significant in the corresponding coherence-squared function.

distinguish between the contributions from local wind forcing within the Indonesian seas and those from the remote wind forcing in the Indian Ocean, we divide the integrated wind stress into different sectors along the entire pathway and reproduce the SLA in the Maluku Channel using the model again: forced by the wind stress only in the western Indian Ocean from (0°, 45°E) to (0°, 75°E) (Figure 10b), only in the eastern Indian Ocean from (0°, 75°E) to (0°, 99°E) (Figure 10c), along the coast of Sumatra and Java from (0°, 99°E) to (9°S, 115.5°E) (Figure 10d), along the 100-m isobath in the Makassar Strait from (9°S, 115.5°E) to (1°N, 120°E) (Figure 10e), and along the coast of north Sulawesi from (1°N, 120°E) to the Maluku Channel (2°N, 126.5°E) (Figure 10f). It is clear that SLA signal at the beginning of 2016 is from the western Indian Ocean (Figure 10b). Two peaks in SLA during October to December 2016 are mainly produced by the wind stress from the eastern Indian Ocean (Figure 10c). In addition, Kelvin wave energy from both the western and eastern Indian Ocean contributes to the amplitude of the SLA from April to August 2016 at the Maluku Channel (Figures 10b and 10c). Alongshore wind along the Sumatra and Java coast and local wind forcing in the Indonesian seas have little contribution to the SLA variability at the Maluku Channel during 2015–2016 on the interannual time scales (Figures 10d–10f).

3.3.2. Coastal Kelvin Waves

Coastal Kelvin waves generated locally within the Sulawesi Sea from the reflection of the Pacific Rossby waves may also play an important role influencing the circulation in the Maluku Channel. To investigate the relationship between the coastal Kelvin waves off the east Philippine coast and the Maluku Channel, we calculate the coherence-squared function of the SLA time series both at the Philippine coast and at the Maluku Channel (Figure 11). The results of the altimetry observation and the INDESO model show that the two are significantly correlated at time scales of 45 days, which is in agreement with the propagation of the first three coastal Kelvin wave modes. Two different pathways around the Sulawesi Sea are possible: (1) The Kelvin wave propagates along the Sulu Archipelago to reach the east Kalimantan coast (Figure 12a) and (2) some of the Kelvin wave energy along the pathway described in pathway (1) might leak into the Sulu Sea via Sibutu Passage (Figure 12b). As we did for the Indian Ocean Kelvin wave pathway, we choose several anchor points along these two waveguides and then calculate the lag correlations between each adjacent point with Aviso SLA (Figures 12c and 12d) and the INDESO model SLA (Figures 12e and 12f). For the Aviso data, the level of correlation along the pathway (1) is high only between point A and point C, and then after point I (Figure 12c). This means that the coastal Kelvin waves may propagate into the Sulawesi Sea but likely do not reach the western edge of the basin. Rather, the Kelvin waves might propagate southward directly through the Sangihe island chain at the entrance of the Sulawesi Sea (see Figure 1a). The correlation between the SLA at the Philippine coast and at the Maluku Channel (e.g., Figure 11) suggests that the SLA

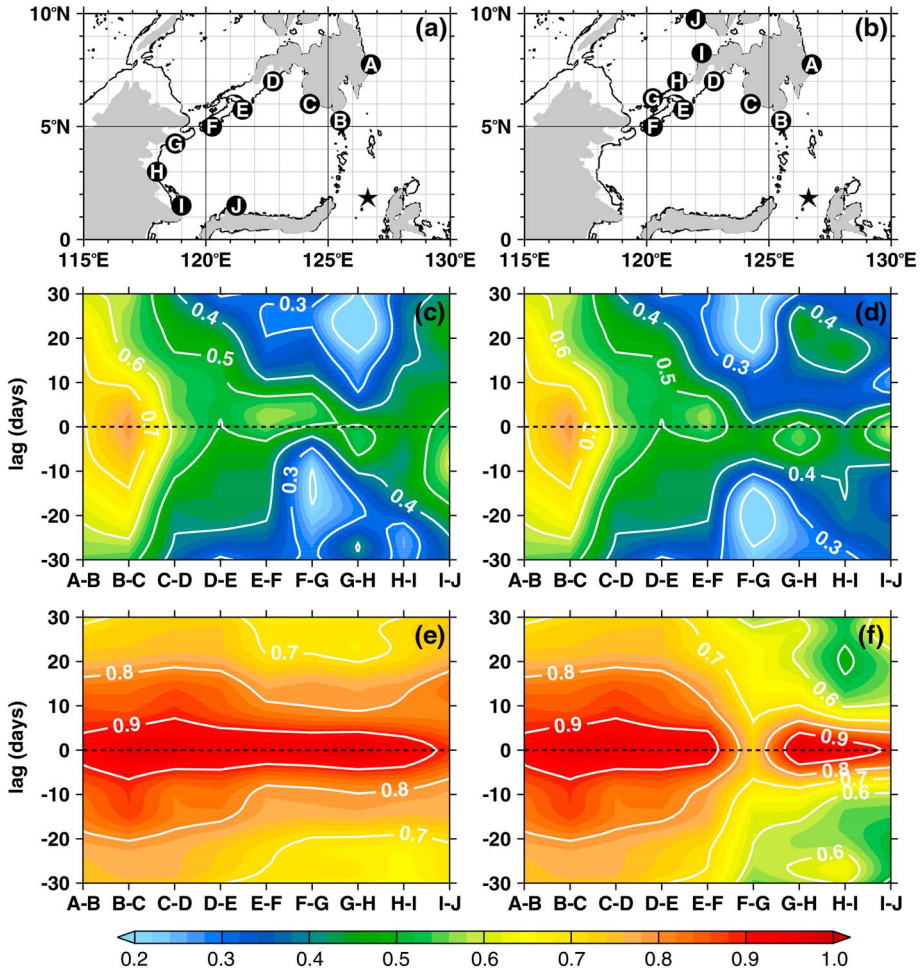

Figure 12. Map of the potential Kelvin wave coastal waveguide pathway from the east coast of the Mindanao island in the Pacific Ocean (point A) through the Sulawesi Sea to (a) northern Sulawesi island or (b) entering the Sulu Sea. Black contours indicate the 100-m isobath. (c) and (d) Lag correlations between points along the possible respective waveguides in Aviso altimeter data. (e) and (f) Same as (c) and (d) but for the INDESO sea level anomaly.

variability could also be impacted by direct advection via the Mindanao Current. In addition, nonlinear dynamics associated with movement of the Mindanao Current retroflection may also drive SLA variability in the Maluku Channel (Yuan, Li, et al., 2018).

In the results of the INDESO model, there exist high correlations at lags of −5 to +5 days with a slight gap between points F and G in the waveguide at the entrance into the Sulu Sea (Figure 12f), although the correlation is still relatively high (0.7) between points F and G. This suggests that most of the coastal Kelvin wave energy that enters into the Sulawesi Sea will bypass the Sibutu Passage and propagate southward along the east Kalimantan coast, then continue to propagate eastward along the northern Sulawesi Sea. The difference between the model results and the Aviso data suggest that the model probably favors the linear wave

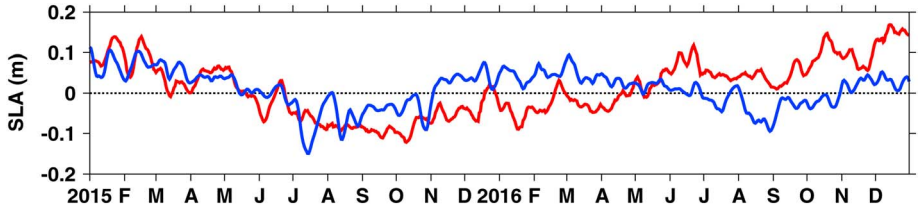

Figure 13. The Aviso sea level anomaly (SLA) at the central Maluku Channel (red curve) and SLA predicted from the Kelvin wave model integrated with wind stress along the coastline of Sulawesi Sea anticlockwise (blue curve).

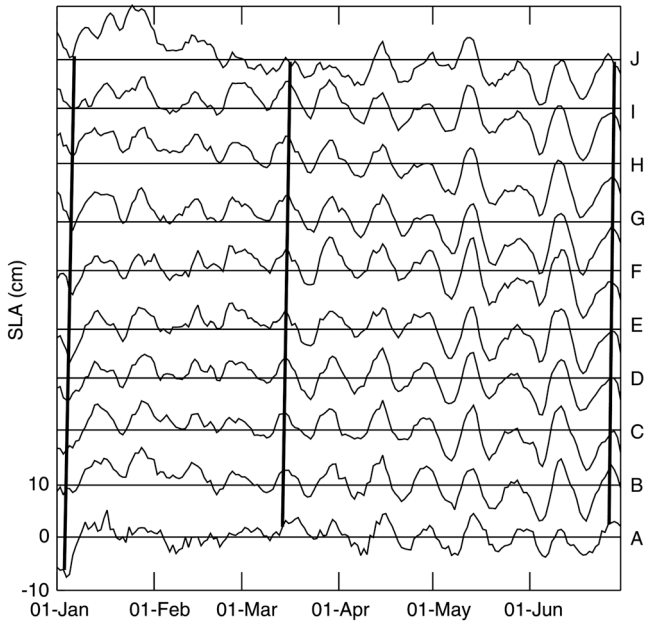

Figure 14. The INDESO sea level anomaly (SLA) at each anchor point along the pathway in Figure 12a during 1 January to 30 June 2015. Each time series is offset by 10 cm in the *y* axis. Thick black lines show the Kelvin wave phase for reference.

dynamics in this region. In addition, the coarse resolution of the altimeter product in the Sulawesi Sea may be another reason for the difference.

We also use the coastally trapped Kelvin wave model to predict the SLA at the Maluku Channel along the pathway shown in Figure 12a. There is remarkably good agreement during the first half year of 2015, especially for the two peaks in February and March (Figure 13). The correlation between the two SLA during this period is as high as 0.80, above the 95% significance level at 0.50 with an effective DOF of 14. This suggests that the coastally trapped Kelvin wave from the North Pacific Ocean can propagate into the Sulawesi Sea and further into the Maluku Channel. The Kelvin wave propagation during this period from January to June 2015 is also clearly indicated in the SLA variations at each point along the pathway in the INDESO model (Figure 14). However, the SLA from the model and from the Aviso data during the remainder of the time series does not compare very well, with a correlation coefficient of 0.18, below the 95% significance level at 0.48 with an effective DOF of 15. This could be because the Pacific variability is blocked by the Mindanao Current retroflection so that the variability in the Maluku Channel during this period is dominated mostly by the Kelvin wave from the Indian Ocean: There is good agreement with the SLA derived from the Kelvin wave model that is integrated from the western Indian Ocean (Figure 10a).

4. Summary

The propagation of planetary waves from both the Indian Ocean and the Pacific Ocean into the Sulawesi Sea was investigated using INDESO model output, mooring observations and linear wave characteristic integration model. The currents reproduced by the INDESO model compared reasonably well with the mooring observations in the upper layer above ~150 m in the Maluku Channel and can explain over 80% of the observational variability. However, in the subsurface between 150 and 400 m, the model overestimates both zonal and meridional velocities. The seasonal cycle of both the model simulation and the observed currents in the Maluku Channel represents annual variabilities in the upper layer and semiannual variabilities in the lower layer separated at about 150 m. However, the subsurface semiannual signal in the model is not so clear in the zonal currents. For the meridional currents, the model semiannual signal lags the observation by about 2 months. Overall, the INDESO model reproduces the general ocean circulation in the upper ocean in the Indonesian seas very well but has notable discrepancies of phase shifts below 150 m.

The interannual variability of the currents from the model suggests a potential relationship with ENSO. The first EOF mode of the interannual variability of the circulation shows that during the El Niño years,

the Mindanao Current flows southward across the entrance of the Sulawesi Sea and joins the Mindanao Eddy-Halmahera Eddy retroflection directly at 2.5°N. During non–El Niño years, the Mindanao Current intrudes into the Maluku Channel southward to 1°S forming a recirculation in the Maluku Sea before rejoining the western boundary current system. The response of the currents at the Maluku Channel to the variabilities of the SLA and the western boundary current of the Pacific Ocean is much more significant than those in the rest of the Indonesian seas like the Makassar Strait, suggesting the important role of the eastern path of the ITF on interannual time scales.

The lag correlation analysis shows strong correlations between SLA in the Maluku Channel and SLA in the Indian Ocean and the western Pacific Ocean. The SLA at the central Maluku Channel predicted by a linear model integrating the wind stress along the Kelvin wave characteristics compared very well to the Aviso SLA when integrated along different waveguides. This suggests that the interannual variability in the Maluku Channel is affected by both the Indian Ocean Kelvin wave energy propagating through the Indonesian seas and the interplay with local coastal Kelvin wave activity within the Sulawesi Sea. Separating the relative contributions of the integrated wind stress forcing into different sectors along the Kelvin wave pathway suggests that the remote wind forcing from the Indian Ocean contributes the most to SLA variability in the central Maluku Channel during the 2015–2016 El Niño, except the first half year of 2015, when the coastally trapped Kelvin wave from the eastern Philippine coast contributes more energy. The flow regime during this time shows no solid intrusion into the Maluku Channel and so also making it easier for the Indian Ocean Kelvin wave to propagate directly into the south Sulawesi Sea. Local wind within the Indonesian seas has little effect on interannual SLA variability in the Maluku Channel.

Acknowledgments
The study was supported by the National Natural Science Foundation of China (NSFC) (41421005, 41720104008, and 41876025), the Strategic Priority Project of the Chinese Academy of Sciences (XDA11010205), the Qingdao National Laboratory for Marine Science and Technology (QNLM) Project (2016ASKJ04), and the Shandong Provincial Project (U1606402). The first author gratefully acknowledges the China Scholarship Council (CSC) support for the Joint Ph.D. Training Program at Scripps Institution of Oceanography, University of California, San Diego. Janet Sprintall was supported by NOAA's Climate Program Office, Climate Variability, and Predictability Program (NA17OAR4310257). Discussion with Lina Yang was very helpful in the course of this work and appreciated. We thank the Indonesian Ministry of Marine Affairs and Fisheries (Kementerian Kelautan dan Perikanan, KKP) for providing the INDESO model output, which can be found at a repository site at Zenodo (https://zenodo.org/record/1411861 and doi:10.5281/zenodo.1411861). The source codes of the NEMO ocean model can be accessed through the website (https://forge.ipsl.jussieu.fr/nemo/svn/NEMO/releases/release-3.6/). The moored ADCP data can be found in the supporting information. More details of the data description and the field experiment can be approached at the website (http://itf.qdio.ac.cn/). The ERA-Interim wind data were obtained from the ECMWF website (https://www.ecmwf.int/en/forecasts/datasets/archive-datasets/reanalysis-datasets/era-interim). The ONI could be found from the CPC website (http://www.cpc.ncep.noaa.gov/data/indices/). The altimeter products were produced by Ssalto/Duacs and distributed by Aviso, with support from CNES (http://www.aviso.altimetry.fr/duacs/). We are also grateful to all the officers and crews of R/V *BJ8* for the successful cruises.

References

Arief, D., & Murray, S. P. (1996). Low-frequency fluctuations in the Indonesian Throughflow through Lombok Strait. *Journal of Geophysical Research*, *101*(C5), 12,455–12,464.

Boulanger, J. P., & Menkes, C. (2001). The Trident Pacific model. Part 2: Role of long equatorial wave reflection on sea surface temperature anomalies during the 1993-1998 TOPEX/POSEIDON period. *Climate Dynamics*, *17*, 175–186.

CLS, S. (2016). SSALTO/DUACS user handbook: MSLA and (M)ADT near-real time and delayed time products. SALP-MU-P-EA-21065-CLS, edition 5.0.

Clarke, A. J. (1991). On the reflection and transmission of low-frequency energy at the irregular western Pacific Ocean boundary. *Journal of Geophysical Research*, *96*(S01), 3289–3305.

Drushka, K., Sprintall, J., Gille, S. T., & Brodjonegoro, I. (2010). Vertical structure of Kelvin waves in the Indonesian Throughflow exit passages. *Journal of Physical Oceanography*, *40*(9), 1965–1987.

Du Penhoat, Y., & Cane, M. A. (1991). Effect of low-latitude western boundary gaps on the reflection of equatorial motions. *Journal of Geophysical Research*, *96*(S01), 3307–3322.

Durland, T. S., & Qiu, B. (2003). Transmission of subinertial Kelvin waves through a strait. *Journal of Physical Oceanography*, *33*, 1337–1350.

Emery, W. J., & Thomson, R. E. (2001). *Data analysis methods in physical oceanography* Waltham, MA: Elsevier Science.

Gill, A. E. (1982). *Atmosphere-ocean dynamics*. San Diego, CA: Academic Press.

Godfrey, J. (1996). The effect of the Indonesian Throughflow on ocean circulation and heat exchange with the atmosphere: A review. *Journal of Geophysical Research*, *101*(C5), 12,217–12,237.

Gordon, A. L. (1986). Interocean exchange of thermocline water. *Journal of Geophysical Research*, *91*(C4), 5037–5046.

Gordon, A. L. (2005). Oceanography of the Indonesian seas and their throughflow. *Oceanography*, *18*(4), 14–27.

Gordon, A. L., Huber, B. A., Metzger, E. J., Susanto, R. D., Hurlburt, H. E., & Adi, T. R. (2012). South China Sea throughflow impact on the Indonesian Throughflow. *Geophysical Research Letters*, *39*, L11602. https://doi.org/10.1029/2012GL052021

Gordon, A., Sprintall, J., Van Aken, H., Susanto, D., Wijffels, S., Molcard, R., et al. (2010). The Indonesian Throughflow during 2004–2006 as observed by the INSTANT program. *Dynamics of Atmospheres and Oceans*, *50*(2), 115–128.

Hu, D., Wu, L., Cai, W., Gupta, A. S., Ganachaud, A., Qiu, B., et al. (2015). Pacific western boundary currents and their roles in climate. *Nature*, *522*, 299–308.

Kashino, Y., Firing, E., Hacker, P., Sulaiman, A., & Lukiyanto (2001). Currents manuscript submitted to JGR: Oceans in the Celebes and Maluku Seas, February 1999. *Geophysical Research Letters*, *28*(7), 1263–1266.

Kessler, W. S., & McCreary, J. P. (1993). The annual wind-driven Rossby wave in the subthermocline equatorial Pacific. *Journal of Physical Oceanography*, *23*(6), 1192–1207.

Kessler, W. S., & McPhaden, M. J. (1995). Oceanic equatorial waves and the 1991–93 El Niño. *Journal of Climate*, *8*(7), 1757–1774.

Koch-Larrouy, A., Madec, G., Bouruet Aubertot, P., Gerkema, T., Bessières, L., & Molcard, R. (2007). On the transformation of Pacific Water into Indonesian Throughflow Water by internal tidal mixing. *Geophysical Research Letters*, *34*, L04604. https://doi.org/10.1029/2006GL028405

Liu, Q., Feng, M., & Wang, D. (2011). ENSO-induced interannual variability in the southeastern South China Sea. *Journal of Oceanography*, *67*(1), 127–133.

Liu, H., Li, W., & Zhang, X. (2005). Climatology and variability of the Indonesian Throughflow in an eddy-permitting oceanic GCM. *Advances in Atmospheric Sciences*, *22*(4), 496–508.

Luick, J. L., & Cresswell, G. R. (2001). Current measurements in the Maluku Sea. *Journal of Geophysical Research*, *106*(C7), 13,953–13,958.

McClean, J. L., Ivanova, D. P., & Sprintall, J. (2005). Remote origins of interannual variability in the Indonesian Throughflow region from data and a global Parallel Ocean Program simulation. *Journal of Geophysical Research*, *110*, C10013. https://doi.org/10.1029/2004JC002477

Meyers, G. (1996). Variation of Indonesian Throughflow and the El Niño–Southern Oscillation. *Journal of Geophysical Research*, *101*(C5), 12,255–12,263.
Murtugudde, R., Busalacchi, A. J., & Beauchamp, J. (1998). Seasonal-to-interannual effects of the Indonesian Throughflow on the tropical Indo-Pacific Basin. *Journal of Geophysical Research*, *103*(C10), 21,425–21,441.
Nugroho, D., Koch-Larrouy, A., Gaspar, P., Lyard, F., Reffray, G., & Tranchant, B. (2017). Modelling explicit tides in the Indonesian seas: An important process for surface sea water properties. *Marine Pollution Bulletin*, *131*, 7–18.
Paek, H., Yu, J.-Y., & Qian, C. (2017). Why were the 2015/2016 and 1997/1998 extreme El Niños different? *Geophysical Research Letters*, *44*, 1848–1856. https://doi.org/10.1002/2016GL071515
Potemra, J. T. (1999). Seasonal variations of upper ocean transport from the Pacific to the Indian Ocean via Indonesian straits. *Journal of Physical Oceanography*, *29*(11), 2930–2944.
Pujiana, K., Gordon, A. L., & Sprintall, J. (2013). Intraseasonal Kelvin wave in Makassar Strait. *Journal of Geophysical Research: Oceans*, *118*, 2023–2034. https://doi.org/10.1002/jgrc.20069
Pujiana, K., Gordon, A. L., Sprintall, J., & Susanto, R. D. (2009). Intraseasonal variability in the Makassar Strait thermocline. *Journal of Marine Research*, *67*(6), 757–777.
Qiu, B., Mao, M., & Kashino, Y. (1999). Intraseasonal variability in the Indo-Pacific Throughflow and the regions surrounding the Indonesian Seas. *Journal of Physical Oceanography*, *29*(7), 1599–1618.
Schneider, N. (1998). The Indonesian Through flow and the global climate system. *Journal of Climate*, *11*(4), 676–689.
Spall, M. A., & Pedlosky, J. (2005). Reflection and transmission of equatorial Rossby waves. *Journal of Physical Oceanography*, *35*(3), 363–373.
Sprintall, J., Gordon, A. L., Koch-Larrouy, A., Lee, T., Potemra, J. T., Pujiana, K., & Wijffels, S. E. (2014). The Indonesian seas and their role in the coupled ocean-climate system. *Nature Geoscience*, *7*(7), 487.
Sprintall, J., Gordon, A. L., Murtugudde, R., & Susanto, R. D. (2000). A semiannual Indian Ocean forced Kelvin wave observed in the Indonesian seas in May 1997. *Journal of Geophysical Research*, *105*(C7), 17,217–17,230.
Sprintall, J., Wijffels, S. E., Molcard, R., & Jaya, I. (2009). Direct estimates of the Indonesian Throughflow entering the Indian Ocean: 2004–2006. *Journal of Geophysical Research*, *114*, C07001. https://doi.org/10.1029/2008JC005257
Susanto, R. D., Ffield, A., Gordon, A. L., & Adi, T. R. (2012). Variability of Indonesian Throughflow within Makassar Strait, 2004–2009. *Journal of Geophysical Research*, *117*, C09013. https://doi.org/10.1029/2012JC008096
Syamsudin, F., Kaneko, A., & Haidvogel, D. B. (2004). Numerical and observational estimates of Indian Ocean Kelvin wave intrusion into Lombok Strait. *Geophysical Research Letters*, *31*, L24307. https://doi.org/10.1029/2004GL021227
Tranchant, B., Reffray, G., Greiner, E., Nugroho, D., Koch-Larrouy, A., & Gaspar, P. (2016). Evaluation of an operational ocean model configuration at 1/12° spatial resolution for the Indonesian seas (NEMO2. 3/INDO12)–Part 1: Ocean physics. *Geoscientific Model Development*, *9*(3), 6611–6668.
White, W. B., Tourre, Y. M., Barlow, M., & Dettinger, M. (2003). A delayed action oscillator shared by biennial, interannual, and decadal signals in the Pacific basin. *Journal of Geophysical Research*, *108*(C3), 3070. https://doi.org/10.1029/2002JC001490
Wijffels, S., & Meyers, G. (2004). An intersection of oceanic waveguides: Variability in the Indonesian Throughflow region. *Journal of Physical Oceanography*, *34*(5), 1232–1253.
Wyrtki, K. (1987). Indonesian through flow and the associated pressure gradient. *Journal of Geophysical Research*, *92*(C12), 12,941–12,946.
Yu, J.-Y., Zou, Y., Kim, S. T., & Lee, T. (2012). The changing impact of El Niño on US winter temperatures. *Geophysical Research Letters*, *39*, L15702. https://doi.org/10.1029/2012GL052483
Yuan, D. (2005). Role of the Kelvin and Rossby waves in the seasonal cycle of the equatorial Pacific Ocean circulation. *Journal of Geophysical Research*, *110*, C04004. https://doi.org/10.1029/2004JC002344
Yuan, D., Hu, X., Xu, P., Zhao, X., Masumoto, Y., & Han, W. (2018). The IOD-ENSO precursory teleconnection over the tropical Indo-Pacific Ocean: dynamics and long-term trends under global warming. *Journal of Oceanology and Limnology*, *36*(1), 4–19.
Yuan, D., Li, X., Wang, Z., Li, Y., Wang, J., Yang, Y., et al. (2018). Observed transport variations in the Maluku Channel of the Indonesian Seas associated with western boundary current changes. *Journal of Physical Oceanography*, *48*(8), 1803–1813.
Yuan, D., Rienecker, M. M., & Schopf, P. S. (2004). Long wave dynamics of the interannual variability in a numerical hindcast of the equatorial pacific ocean circulation during the 1990s. *Journal of Geophysical Research*, *109*, C05019. https://doi.org/10.1029/2003JC001936
Yuan, D., Wang, J., Xu, T., Xu, P., Hui, Z., Zhao, X., et al. (2011). Forcing of the Indian Ocean Dipole on the interannual variations of the tropical Pacific Ocean: Roles of the Indonesian Throughflow. *Journal of Climate*, *24*(14), 3593–3608.
Yuan, D., Zhou, H., & Zhao, X. (2013). Interannual climate variability over the tropical Pacific Ocean induced by the Indian Ocean Dipole through the Indonesian Throughflow. *Journal of Climate*, *26*(9), 2845–2861.